Microbunching Instability in Relativistic Electron Bunches: Direct Observations of the Microstructures Using Ultrafast YBCO Detectors

E. Roussel, C. Evain, C. Szwaj, and S. Bielawski
Laboratoire de Physique des Lasers, Atomes et Molécules (PhLAM), UMR CNRS 8523, Centre d'Études et de Recherches Lasers et Applications (CERLA), Université Lille 1, F-59655 Villeneuve d'Ascq Cedex, France

J. Raasch, P. Thoma, A. Scheuring, M. Hofherr, K. Ilin, S. Wünsch, and M. Siegel
Institute of Micro- and Nanoelectronic Systems, Karlsruhe Institute of Technology (KIT), 76187 Karlsruhe, Germany

M. Hosaka, N. Yamamoto, and Y. Takashima
Graduate School of Engineering, Nagoya University, Nagoya 464-8603, Japan

H. Zen
Institute of Advanced Energy, Kyoto University, Uji 611-0011, Japan

T. Konomi, M. Adachi, S. Kimura, and M. Katoh
UVSOR Facility, Institute for Molecular Science, National Institutes of Natural Sciences, Okazaki 444-8585, Japan
(Received 27 January 2014; published 25 August 2014)

Relativistic electron bunches circulating in accelerators are subjected to a dynamical instability leading to microstructures at millimeter to centimeter scale. Although this is a well-known fact, direct experimental observations of the structures, or the field that they emit, remained up to now an open problem. Here, we report the direct, shot-by-shot, time-resolved recording of the shapes (including envelope and carrier) of the pulses of coherent synchrotron radiation that are emitted, and that are a "signature" of the electron bunch microstructure. The experiments are performed on the UVSOR-III storage ring, using electrical field sensitive $YBa_2Cu_3O_{7-x}$ thin-film ultrafast detectors. The observed patterns are subjected to permanent drifts, that can be explained from a reasoning in phase space, using macroparticle simulations.

DOI: 10.1103/PhysRevLett.113.094801 PACS numbers: 41.60.Ap, 05.45.-a, 29.27.Bd

Relativistic electron bunches are known to interact with their own electromagnetic fields in a nontrivial way, in particular when they are deviated by a magnetic field, or when conducting walls are present in their vicinity. This is the cause of a striking phenomenon leading to the spontaneous formation of a structure in the longitudinal dimension of the electron bunch: the so-called microbunching instability [1–3]. This represents one of the most fundamental limitations of stable operation in electron storage rings, as well as a means to produce high intensity coherent radiation. This effect is observed and studied in a wide range of storage ring facilities, such as ALS [3], ANKA [4], BESSY [5], DIAMOND [6], ELETTRA [7], MLS [8], Synchrotron SOLEIL [9], and UVSOR [10].

However, comparisons between models and experiments have been up to now indirect. Indeed, experimental data have been essentially based on the recordings of the pulses of millimeter wave coherent emission (coherent synchrotron radiation or CSR), using a bolometer or a diode detector at a terahertz (THz) beam line. Because of the relatively slow response time of these detection systems, only the evolution of the pulse energy could be monitored, and real-time monitoring of the pulse shape evolution was unfortunately out of reach. Time-resolved recordings using electro-optic sampling have also shown to be possible [11], though the low repetition rate of these devices does not allow us yet to monitor the dynamical microstructure evolution over several turns.

In this Letter, we demonstrate the possibility to monitor the microstructure dynamics in real time (turn-by-turn), when the electron bunch duration exceeds several tens of picoseconds, using a new generation of ultrafast detectors based on thin films of the high-temperature superconductor $YBa_2Cu_3O_{7-x}$ (YBCO) [12–14]. Indeed, the temporal resolution of these detectors is only limited by the bandwidth of readout electronics and oscilloscope speed (16 ps FWHM here), and thus allows us to record details of the emitted CSR pulses. Furthermore, full characterization of the CSR pulses (amplitude and carrier) can be carried out, because those detectors are directly sensitive to the electric field.

In the first part, we present a study of the dynamics above the microbunching instability, and interpret the pattern dynamics from the phase space motion. In the second step, we also present the response of the electron bunch when the CSR instability is seeded [15] by a localized laser perturbation.

The experimental arrangement is displayed in Fig. 1. The UVSOR-III storage ring is operated in single bunch mode

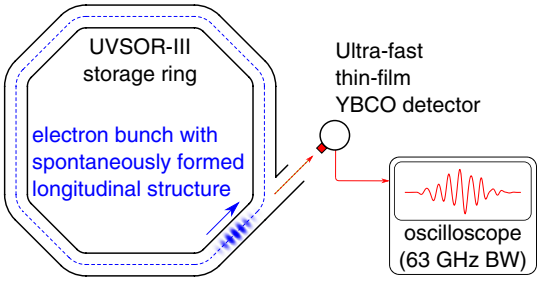

FIG. 1 (color online). Scheme of the experiment. A relativistic electron bunch is stored in the UVSOR-III storage ring. When the electron bunch density exceeds a given threshold, a dynamical instability leads to the spontaneous formation of a pattern in the longitudinal direction. In this Letter, the coherent emission (with ≈9 mm wavelength) due to the presence of the structure is directly monitored, using a new type of thin-film superconducting detector based on YBCO (see text).

above the threshold for microbunching instability, at a current of 60 to 65 mA. In these conditions, coherent millimeter wave radiation is emitted in the bending magnets, which is a signature of a modulation of the electron bunch at millimeter scale. At the output port of the BL6B THz beam line [16,17], we placed the thin-film YBCO detector, described in detail in Refs. [12–14]. It was operated at liquid nitrogen temperature without any bias. The detector was positioned near the focusing point of the beam line, and the signal was directly recorded by a 63 GHz oscilloscope (Agilent DSOX96204Q) without any amplification.

The coherent synchrotron radiation is composed of a series of pulses [Fig. 2(b)], each having a duration of the order of 300 ps, separated by the storage-ring round-trip time (177 ns). The envelope was found to vary slowly (near threshold), or in a bursting manner far from threshold [Fig. 2(a)]. The first observation of typical single pulses [Fig. 2(c)] revealed that the electric field evolution, including the optical carrier, could be directly observed by the YBCO detection system and that the carrier frequency was in the 1 cm^{-1} range.

Then we proceeded to systematic recordings of long time series above the microbunching instability threshold. We summarized their dynamical evolutions as a color map versus a "fast time" (i.e., resolving the pulse shape), and a "slow time" (associated to the number of round-trips). All data displayed a systematic pattern [Fig. 2(d)], with two visible parts. The first one is a structure at the bunch head [in the lower part of Fig. 2(d), before ≈125 ps], which systematically drifts towards the tail. The second part (after ≈125 ps) is constituted of a combination of two structures that move in both directions.

These two directions of motion can be interpreted from a reasoning in the phase space of the electrons. Assuming that the relevant motion occurs in the longitudinal direction [1–3], the state of each electron i at time t is defined by its instantaneous position $z_i(t)$ and an energy variable $\delta_i(t)$. The dynamics of the electrons can be described by the following model [18,19]:

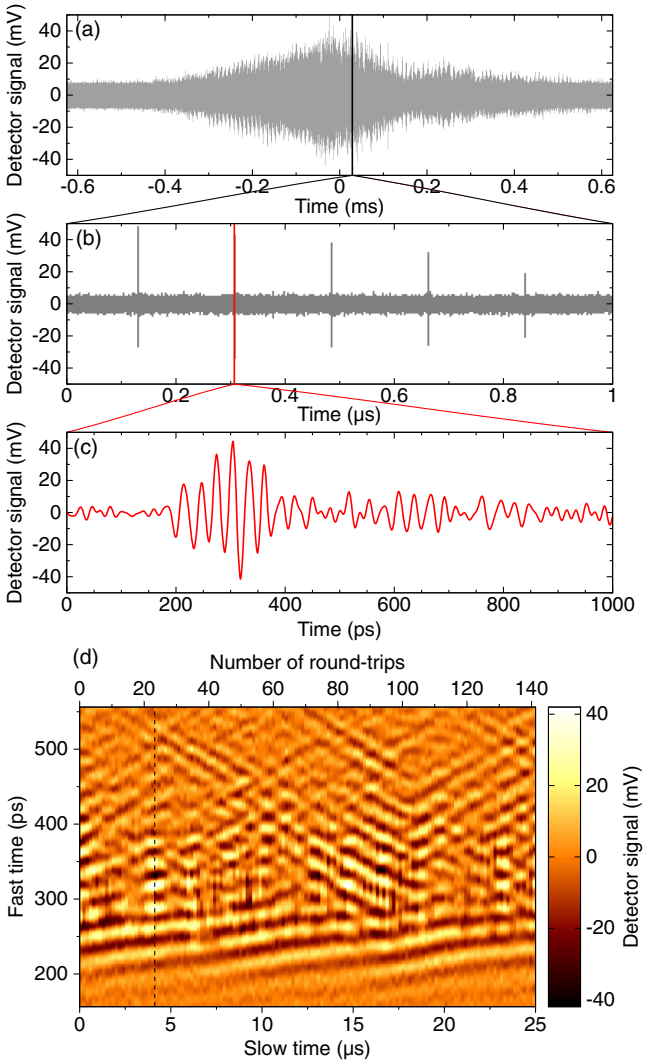

FIG. 2 (color online). Typical shape of a single pulse that is detected by the YBCO ultrafast detector (in red). (a), (b), and (c) represent the same signal at different scales. The color scale diagram (d) represents the evolution of the (c) signal over many successive turns in the storage ring. Note that the voltage is directly proportional to the electric field of the incoming radiation, and that both the envelope and the carrier are thus recorded. The dashed line in (d) corresponds to the signal displayed in (c).

$$\frac{dz_i}{dt} = -\eta c \delta_i \tag{1}$$

$$\frac{d\delta_i}{dt} = -\left(\frac{\omega_s^2}{\eta c}\right) z_i - \left(\frac{2}{\tau_s}\right) \delta_i - F - \eta_n \xi(t), \tag{2}$$

where t is a continuous time variable corresponding to the number of round-trips (i.e., the slow time variable in Fig. 2). $\delta_i(t) = [E_i(t) - E_R]/E_R$, where E_i and E_R are, respectively, the electron energy and a reference energy of the storage ring (600 MeV here). $\omega_s/2\pi$ is a dynamical frequency called the synchrotron frequency (23.1 kHz here,

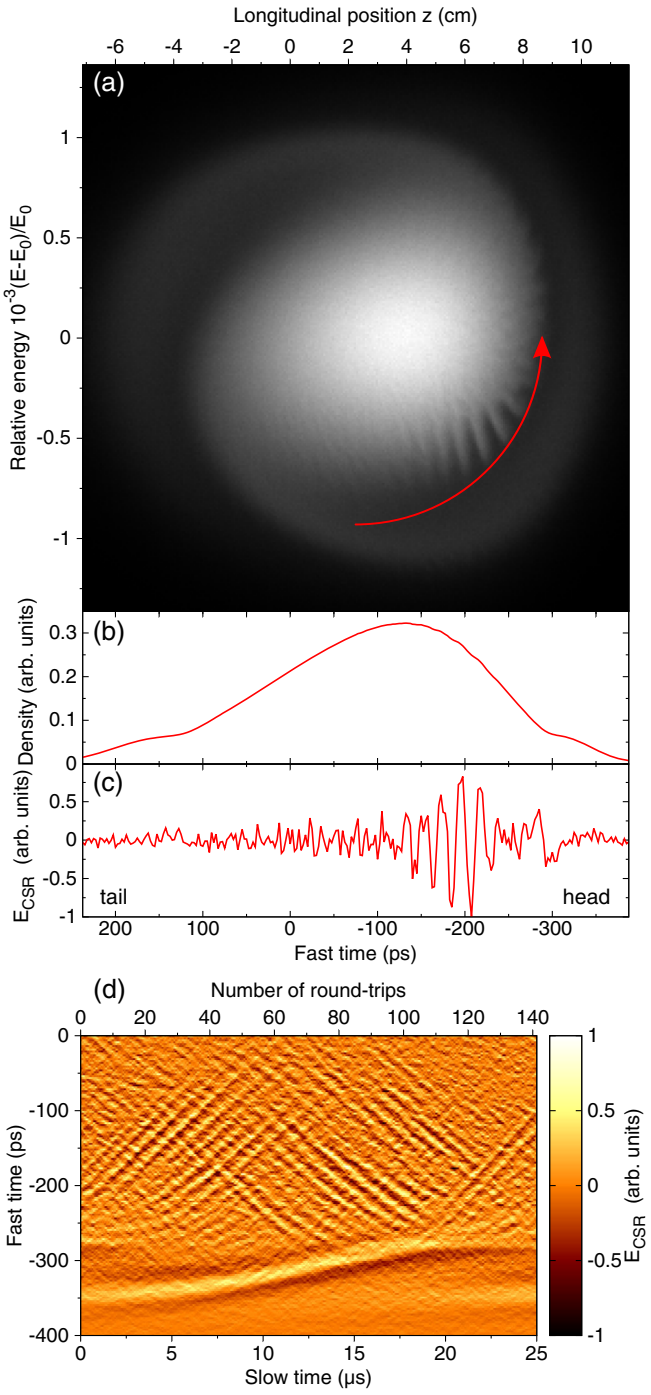

FIG. 3 (color online). Interpretation of the drifting motions observed in Fig. 2(d), from the model (2). (a) Distribution of the electrons in longitudinal phase space (position z energy δ) at a given time. The CSR instability leads to a microstructure in this phase space. (b) Longitudinal electron density distribution, i.e., obtained by the vertical projection of the distribution (a). (c) CSR electric field deduced from (b). Note that the structure is more clearly observable in (c) than in (b), because slow variations are cut off in the CSR process. The electric field versus time (d) reveals that the structures are permanently drifting, as in the experiment. This is essentially due to the permanent rotation of the electron distribution (a) at the synchrotron frequency.

not to be confused with the revolution frequency in the ring). τ_s is the synchrotron damping time. η is a parameter measuring the dependence of the round-trip length with the energy. The term $\eta_n \xi(t)$ accounts for the stochastic fluctuations of the synchrotron losses. $\xi(t)$ is a Gaussian noise with $\langle \xi(t)\xi(t')\rangle = \delta(t-t')$. F characterizes the collective force exerted on electron i by the other electrons. Parameters, the expression of F, and integration details are given in the Supplemental Material [20].

The link between the electron phase space distribution and the data provided by the detector is presented in Fig. 3. Pattern formation occurs in the electron density distribution, which we will name $f(z,\delta,t)$ [Fig. 3(a)]. However, only the projection on the z coordinate

$$\rho(z,t) = \int_{-\infty}^{-\infty} f(z,\delta,t)d\delta, \tag{3}$$

which corresponds to the longitudinal shape of the electron bunch, is relevant to the observations [Fig. 3(b)]. In this projection, it is clear that the modulation due to the microstructure is extremely weakly contrasted compared to the "global shape" of the electron bunch. Nevertheless this modulation is crucial as it leads to the CSR field [Fig. 3(c)] that is observed experimentally. A typical evolution of this electric field during a CSR burst is represented Fig. 3(d) [with the same color scale representation as the experimental diagram in Fig. 2(d)].

The directions of drifts observed experimentally in Fig. 2(d) can be interpreted from the motion of the electron bunch distribution in phase space $f(z,\delta,t)$. Indeed this distribution [Fig. 3(a)] is subjected to a global rotation near the frequency $\omega_s/2\pi$ (23.1 kHz for our experiment). Hence, globally speaking, the structures drifting toward the bunch head in Figs. 2(d) and 3(d) correspond to structures that are present in the lower part of phase space [Fig. 3(a)], and vice versa.

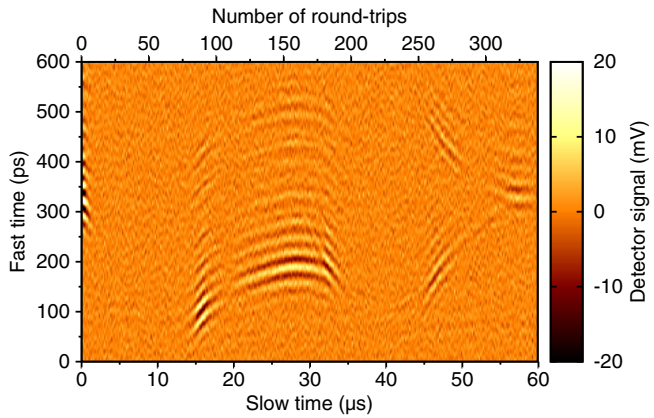

FIG. 4 (color online). Dynamics following a localized laser perturbation (slicing) at $t = 0$, when the system is below the instability threshold. Note that no CSR emission is detected before $t < 0$. Interpretations are given in Fig. 5.

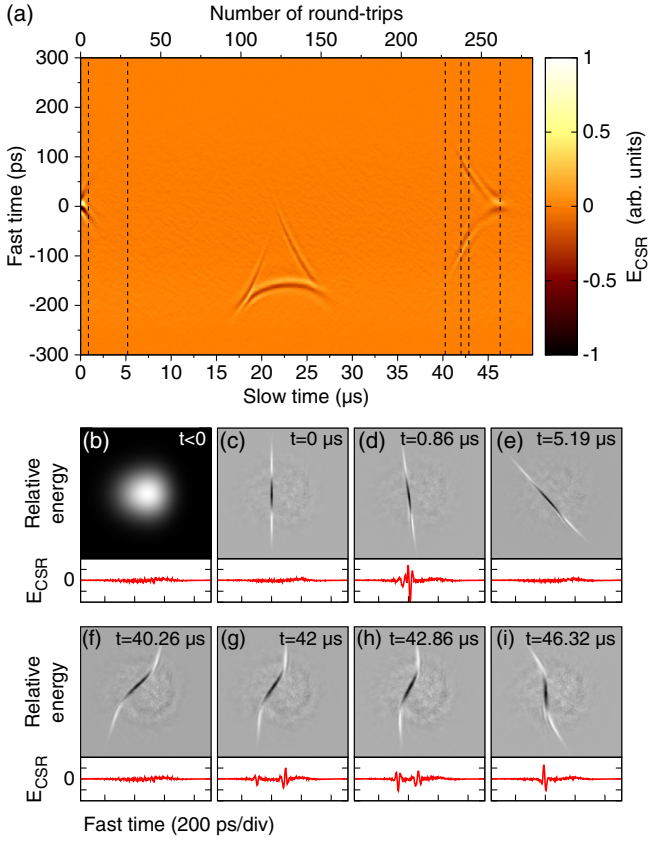

FIG. 5 (color online). Numerical simulation of transients after slicing the electron bunch with a laser, and interpretation in phase space. (a) Simulation of the detection signals. (b)–(i) Phase-space distribution (grayscale image) and associated CSR wakefield (red curve) at different times. For clarity, the reference distribution before laser perturbation (b) is subtracted from the distributions. (c),(d),(e), snapshots near $t = 0$. (f),(g),(h), and (i) are successive snapshots corresponding to different instants of the "cusp" feature visible in (a) at $t = 40$–47 μs.

The phase space dynamics can also be studied below the microbunching instability threshold, by examining the response to a perturbation to a short laser pulse. The experimental response presented in Fig. 4 is obtained using a 15 ps pulse from a titanium-sapphire laser (800 nm, 10 mJ, with an adjustable grating pulse compressor [26]), interacting with the electron bunch in an undulator [16], and the corresponding simulation is displayed in Fig. 5(a). The data recorded by the YBCO detector display characteristic features, as the cusp (or "Y shape") present at the right of the color scale diagrams. These features can be also understood from the examination of the phase space versus time [Figs. 5(c)–(i)] and the associated CSR wakefields. From this chronology, we can see that the cusp appears as a signature of the transformation of the initially straight slice [Fig. 5(c)] into an "S-shaped" slice. It is observed that the peak response occurs when the inflexion point of the S shape is nearly vertical. The two branches of the cusp correspond to the progressive merging of the two pulses [red curves in Figs. 5(g) and 5(h)], each being associated with nearly vertical parts of the S-shaped slice (phase-space plots in Fig. 5).

In conclusion, we showed that using a YBCO thin-film superconducting detector sensitive to the electrical field it is now possible to investigate in detail the CSR pulses at millimeter-centimeter wavelengths, which result from the microbunching instability. The actual time scales of the experiment allowed us to record the carrier and envelope of pulses, thus, allowing us to analyze the chaotic evolutions of the bursts in a very detailed way. Extension of this detection method can be also performed in cases where the carrier cannot be resolved, by biasing the detector. In this case, only the pulses' envelopes can be recorded [14], but at a similar speed. More generally, we believe that this new detector technology will allow us to probe the validity of existing and future models, which differ in particular by the way to approximate the evolution equation (as the Vlasov versus macroparticle approach) and by the numerous possibilities for the wakefield modeling [27].

We would like to thank Agilent, LeCroy, and Tektronix, for providing the oscilloscopes needed for the ultrafast data acquisition. The work was supported by the Joint Studies Program of the Institute for Molecular Science, the JSPS fellowship program for research in Japan (S-09171), the Projet International de Coopération Scientifique PICS project from CNRS, the Grant-in-aid for scientific researches (B20360041) of JSPS, the ANR (Blanc 2010-042301), and used HPC resources from GENCI TGCC/IDRIS (2013-x2013057057, 2014x2014057057). The CERLA is supported by the French Ministère chargé de la Recherche, the Région Nord-Pas de Calais and the FEDER. The KIT is supported in part by the German Federal Ministry of Education and Research under Grant No. 05K2010.

[1] M. Venturini and R. Warnock, Phys. Rev. Lett. **89**, 224802 (2002).
[2] G. Stupakov and S. Heifets, Phys. Rev. ST Accel. Beams **5**, 054402 (2002).
[3] J. M. Byrd, W. P. Leemans, A. Loftsdottir, B. Marcelis, M. C. Martin, W. R. McKinney, F. Sannibale, T. Scarvie, and C. Steier, Phys. Rev. Lett. **89**, 224801 (2002).
[4] V. Judin, N. Hiller, A. Hofmann, E. Huttel, B. Kehrer, M. Klein, S. Marsching, C. Meuter, A.-S. Mueller, M. J. Nasse, M. Schuh, M. S. N. Smale, and M. I. Streichertin, in *Proceedings of the International Particle Accelerator Conference, New Orleans, USA,* (IPAC'12 OC/IEEE, and the Joint Accelerator Conferences Website (JACoW), CERN, Geneva, 2012), TUPPP010, p. 4761.
[5] M. Abo-Bakr, J. Feikes, K. Holldack, G. Wüstefeld, and H.-W. Hübers, Phys. Rev. Lett. **88**, 254801 (2002).
[6] W. Shields, R. Bartolini, G. Boorman, P. Karataev, A. Lyapin, J. Puntree, and G. Rehm, J. Phys. Conf. Ser. **357**, 012037 (2012).
[7] E. Karantzoulis, G. Penco, A. Perucchi, and S. Lupi, Infrared Phys. **53** 300 (2010).

[8] G. Wüstefeld, J. Feikes, M. V. Hatrott, M. Ries, A. Hoehl, R. Klein, R. üller, A. Serdyukov, and G. Ulm, in *Proceedings of the International Particle Accelerator Conference, Kyoto, Japan* (IPAC'10 OC/ACFA and the Joint Accelerator Conferences Website (JACoW), CERN, Geneva, (2010), WEPEA015, p. 2508.

[9] C. Evain, J. Barros, A. Loulergue, M. A. Tordeux, R. Nagaoka, M. Labat, L. Cassinari, G. Creff, L. Manceron, J. B. Brubach, P. Roy, and M. E. Couprie, Europhys. Lett. **98**, 40 006 (2012).

[10] Y. Takashima, M. Katoh, M. Hosaka, A. Mochihashi, S.-I. Kimura, and T. Takahashi, Jpn. J. Appl. Phys. **44**, L1131 (2005).

[11] N. Hiller, A. Borysenko, E. Hertle, E. Huttel, V. Judin, B. Kehrer, S. Marsching, A.-S. Mller, M. Nasse, A. Plech, M. Schuh, and S. Smale, in *Proceedings of the International Particle Accelerator Conference, Shanghai, China* (IPAC'13 OC and the Joint Accelerator Conferences Website (JACoW), CERN, Geneva, 2013), MOPME014, p. 500.

[12] P. Thoma, A. Scheuring, M. Hofherr, S. Wünsch, K. Il'in, N. Smale, V. Judin, N. Hiller, A.-S. Müller, A. Semenov, H.-W. Hübers, and M. Siegel, Appl. Phys. Lett. **101** 142601 (2012).

[13] P. Probst, A. Semenov, M. Ries, A. Hoehl, P. Rieger, A. Scheuring, V. Judin, S. Wunsch, K. Ilin, N. Smale, Y.-L. Mathis, R. Muller, G. Ulm, G. Wustefeld, H.-W. Hubers, J. Hanisch, B. Holzapfel, M. Siegel, and A.-S. Muller, Phys. Rev. B **85**, 174511 (2012).

[14] P. Thoma, A. Scheuring, S. Wunsch, K. Il'in, A. Semenov, H. Hubers, V. Judin, A.-S. Muller, N. Smale, M. Adachi, S. Tanaka, A. Kimura, M. Katoh, N. Yamamoto, M. Hosaka, E. Roussel, C. Szwaj, S. Bielawski, and M. Siegel, IEEE Trans. Terahertz Sci. Technol. **3**, 81 (2013).

[15] J. M. Byrd, Z. Hao, M. C. Martin, D. S. Robin, F. Sannibale, R. W. Schoenlein, A. A. Zholents, and M. S. Zolotorev, Phys. Rev. Lett. **97**, 074802 (2006).

[16] M. Adachi, H. Zen, T. Konomi, J. Yamazaki, K. Hayashi, and M. Katoh, J. Phys. Conf. Ser. **425**, 042013 (2013).

[17] S. Kimura, E. Nakamura, T. Nishi, Y. Sakurai, K. Hayashi, J. Yamazaki, and M. Katoh, Infrared Phys. **49**, 147 (2006).

[18] *Physics of Collective Beam Instabilities in High Energy Accelerators*, edited by A. W. Chao (Wiley, New York, 1993).

[19] M. Bai, D. Jeon, S. Y. Lee, K. Y. Ng, A. Riabko, and X. Zhao, Phys. Rev. E, **55**, 3493 (1997).

[20] See Supplemental Material at http://link.aps.org/supplemental/10.1103/PhysRevLett.113.094801 for modeling and numerical integration details, which includes Refs. [21–25].

[21] *Accelerator Physics and Engineering*, edited by A. W. Chao and M. Tigner (World Scientific, Singapore, 1999).

[22] R. Warnock, K. Bane, and J. Ellison, in *Proceedings of the European Particle Accelerator Conference, Vienna, Austria* (IPAC'12 OC/IEEE and the Joint Accelerator Conferences Website (JACoW), CERN, Geneva, 2000), WEP2A12, p. 1182.

[23] I. Martin, C. Thomas, R. Bartolini, and J. Adams, in *Proceedings of the International Particle Accelerator Conference, New Orleans, USA* (IPAC'12 OC/IEEE, and the Joint Accelerator Conferences Website (JACoW), CERN, Geneva, 2012), TUPPP031, p. 1677.

[24] E. Roussel, C. Evain, C. Szwaj, and S. Bielawski, Phys. Rev. ST Accel. Beams **17**, 010701 (2014).

[25] R. L. Honeycutt, Phys. Rev. A **45**, 600 (1992).

[26] M. Hosaka, N. Yamamoto, Y. Takashima, C. Szwaj, M. Le Parquier, C. Evain, S. Bielawski, M. Adachi, H. Zen, T. Tanikawa, S. Kimura, M. Katoh, M. Shimada, and T. Takahashi, Phys. Rev. ST Accel. Beams **16**, 020701 (2013).

[27] G. Bassi, T. Agoh, M. Dohlus, L. Giannessi, R. Hajima, A. Kabel, T. Limberg, and M. Quattromini, Nucl. Instrum. Methods Phys. Res., Sect. A **557**, 189 (2006).